

Geochemistry, Geophysics, Geosystems



RESEARCH ARTICLE

10.1029/2021GC009940

Key Points:

- Phytoplankton biomarkers indicate lower primary productivity in the East Siberian Sea than in the West-Chukchi Sea
- Continental run-off can bias PIP₂₅ based sea-ice estimates in marginal seas
- Strongest correlation was found between P_{III}IP₂₅ and summer sea ice at locations remote from river run-off influence

Supporting Information:

Supporting Information may be found in the online version of this article.

Correspondence to:

J. Ren, J. Chen, jian.ren@sio.org.cn; jfchen@sio.org.cn

Citation:

Su, L., Ren, J., Sicre, M.-A., Bai, Y., Jalali, B., Li, Z., et al. (2022). HBIs and sterols in surface sediments across the East Siberian Sea: Implications for palaeo sea-ice reconstructions. *Geochemistry, Geophysics, Geosystems*, 23, e2021GC009940. https://doi.org/10.1029/2021GC009940

Received 2 JUN 2021 Accepted 10 JAN 2022

Author Contributions:

Conceptualization: Liang Su, Jian Ren, Marie-Alexandrine Sicre, Jianfang Chen Funding acquisition: Jian Ren, Youcheng Bai, Zhongqiao Li, Anatolii S. Astakhov, Xuefa Shi, Jianfang Chen Investigation: Liang Su, Jian Ren Methodology: Liang Su, Jian Ren, Marie-Alexandrine Sicre, Youcheng Bai, Bassem Jalali

Project Administration: Haiyan Jin,

© 2022. The Authors.

Jianfang Chen

This is an open access article under the terms of the Creative Commons Attribution-NonCommercial-NoDerivs License, which permits use and distribution in any medium, provided the original work is properly cited, the use is non-commercial and no modifications or adaptations are made.

HBIs and Sterols in Surface Sediments Across the East Siberian Sea: Implications for Palaeo Sea-Ice Reconstructions

Liang Su^{1,2}, Jian Ren², Marie-Alexandrine Sicre³, Youcheng Bai², Bassem Jalali^{2,3}, Zhongqiao Li², Haiyan Jin^{2,4}, Anatolii S. Astakhov⁵, Xuefa Shi⁶, and Jianfang Chen^{2,4}

¹Ocean College, Zhejiang University, Zhoushan, China, ²Key Laboratory of Marine Ecosystem Dynamics, Second Institute of Oceanography, Ministry of Natural Resources, Hangzhou, China, ³Sorbonne Université, Pierre et Marie Curie, CNRS, LOCEAN, Paris, France, ⁴State Key Laboratory of Satellite Ocean Environment Dynamics, Second Institute of Oceanography, Ministry of Natural Resources, Hangzhou, China, ⁵V.I. Il'ichev Pacific Oceanological Institute, Far Eastern Branch of Russian Academy of Sciences, Vladivostok, Russia, ⁶Key Laboratory of Marine Geology and Metallogeny, First Institute of Oceanography, Ministry of Natural Resources, Qingdao, China

Abstract Highly branched isoprenoids (HBIs) in marine sediments have emerged as promising semi-quantitative proxies to reconstruct seasonal sea ice in polar oceans. In this work, we examine the distribution of sympagic HBIs (IP₂₅ and HBI-II), pelagic phytoplankton biomarkers (brassicasterol, dinosterol and HBI-III) as well as terrestrial sterols (campesterol and β-sitosterol) in the surface sediments of the East Siberian Sea (ESS) to test their reliability as sea-ice proxies under continental run-off influence. Our data suggest that dinosterol performs better than brassicasterol to assess sea ice across the ESS shelf, yet the correlation between P_DIP_{25} and spring sea ice is relatively weak but improves when removing sites with salinity <25. Strongest relationship is found between $P_{III}IP_{25}$ and summer sea ice in regions remote from riverine influence. Overall, our results show that semi-quantitative estimates of sea ice based on biomarkers can be problematic in Arctic Ocean margins because of biases induced by continental run-off on biological productivity and sea-ice production.

Plain Language Summary Biomarkers in sediments provide information on past surface water environmental and biological conditions. They show that primary production in the West-Chukchi Sea is higher than in the East Siberian Sea due to sea-ice retreat as a result of global warming and nutrient-rich Pacific water inflow. They also emphasize that sea-ice estimates in continental shelf sediments can be biased by continental run-off.

1. Introduction

Since the beginning of the twentieth century, the global ocean has undergone unprecedented changes caused by global warming (Gillett et al., 2021; Stocker et al., 2013). These changes are notably pronounced in the Arctic region due to polar amplification with major consequences for sea-ice cover and the thermohaline circulation (Cavalieri et al., 1997; Shindell & Faluvegi, 2009). The Arctic Ocean and its marginal seas are characterized by large seasonal sea-ice changes. Melting in summer and sea-ice formation in winter, including coastal polynyas, through the production of cold and saline waters, alter deep-water formation and subsequently the Arctic Ocean circulation (Arrigo, 2014; Cai et al., 2010; Overland & Wang, 2013; Xiao et al., 2013). At the current rate of decline (0.42% year⁻¹), the Arctic Ocean may be ice-free in summer season in the next 50 or even 30 years (Comiso, 2012; Wang et al., 2019), which will profoundly impact the global climate and carbon cycle and further accelerate global warming causing damages to the polar ecosystems (Moline et al., 2008). In Arctic marginal seas changes in sea-ice cover and thickness involve different thermodynamic and dynamic factors (Polyakov et al., 2003). In the case of the East Siberian Sea (ESS), land run-off and atmospheric circulation are controlling factors of the sea-ice distribution (Park et al., 2020; Rigor & Wallace, 2004).

Our knowledge on natural variability of Arctic sea ice and on-going changes are limited by the lack of long time series observations. Information on past sea-ice distribution can be obtained from micropaleontological fossils (Cronin et al., 2013; de Vernal et al., 2020; Nair et al., 2019), geochemical indexes (Hillaire-Marcel & de Vernal, 2008) or biomarker proxies such as IP_{25} (Ice Proxy with 25 carbon atoms), a mono-unsaturated highly branched isoprenoid (HBI) produced by sea-ice diatoms (Belt et al., 2007). Although known modern producers of IP_{25} only account for ~3.6% of the total diatoms living in the Arctic (Brown et al., 2014), a significant positive correlation between sea-ice diatoms and sympagic IP_{25} has been found in the sediment trap data from the

SU ET AL. 1 of 14



Resources: Jian Ren, Zhongqiao Li, Anatolii S. Astakhov, Xuefa Shi, Jianfang Chen

Supervision: Jian Ren

Writing – original draft: Liang Su, Jian Ren, Marie-Alexandrine Sicre, Youcheng Bai, Bassem Jalali

Writing – review & editing: Jian Ren, Marie-Alexandrine Sicre, Youcheng Bai, Bassem Jalali, Zhongqiao Li, Haiyan Jin, Anatolii S. Astakhov, Xuefa Shi, Jianfang Chen western Arctic Ocean (Fahl & Nöthig, 2007; Ren et al., 2020; Zernova et al., 2000). Since the first IP₂₅-based sea-ice reconstruction of Massé et al. (2008) off North Iceland, the PIP₂₅ (Phytoplankton-IP₂₅) index combining IP25 with phytoplankton markers (brassicasterol or dinosterol) has been proposed to derive semi-quantitative estimates of sea ice (Müller et al., 2011). More recently, the substitution of sterols by the tri-unsaturated HBI alkene (HBI-III) in the PIP₂₅ index has been proposed to better reflect ice-free pelagic phytoplankton than sterols (Bai et al., 2019; Koch et al., 2020; Smik, Cabedo-Sanz, & Belt, 2016). Numerous studies have been carried out to produce past sea-ice reconstructions (for reviews and further references see Belt, 2018; Belt & Müller, 2013; Stein et al., 2012) including in the Arctic Ocean (Belt, 2018; Belt & Müller, 2013; Stein et al., 2016, 2017; Xiao, Stein, & Fahl, 2015). The applicability of HBIs and sterols in the pan-Arctic surface sediments for assessing (paleo) sea ice has also been discussed (Kolling et al., 2020; Stoynova et al., 2013; Xiao, Fahl, et al., 2015). Yet, the production, export and preservation of HBIs are still poorly documented and require further investigations to achieve robust sea-ice reconstructions. In this regard, although the influence of continental run-off on the HBIs and phytosterol production and its impact on PIP25 values has been initially discussed in Hörner et al. (2016) and Xiao et al. (2013), uncertainties remain due to the lack of observations. This study presents a mapping of HBIs and sterol concentrations in 42 surface sediments from the ESS and adjacent West-Chukchi Sea (thereafter West-CS; see Figure 1) and assess existing proxies of seasonal sea ice under high continental run-off.

2. Regional Settings

The ESS is one of the heaviest sea ice covered marginal seas of the Eurasian continent. It is largely influenced by both Eurasian rivers run-off and the Arctic Oscillation (AO) which in turn modulate the ocean circulation over most of the basin (Dukhovskoy et al., 2006; Thompson & Wallace, 1998). The water circulation in the ESS consists of the Siberian Coastal Current (SCC) that runs alongshore from west to east, the Pacific Water Inflow (PWI) through the Bering Strait (BS) and the discharge of two large rivers, the Indigirka River (IR) and the Kolyma River (KR; Münchow et al., 1999; Figure 1). Originated from the Laptev Sea (LS) through the Dmitry Laptev Strait, the SCC flows eastwards into the ESS and mixes on its path with Siberian river freshwaters and sea-ice melt waters. Forced by winds, the SCC continues and crosses the Long Strait before dissipating in the CS (Weingartner et al., 1999). When entering the Arctic Ocean, the PWI splits into three branches: the western branch Anadyr Water (AW, high salinity and high-nutrient), the middle branch Bering Shelf Water (BSW, medium salinity), and the eastern branch Alaskan Coastal Water (ACW, low salinity and low-nutrient; Coachman & Aagaard, 1966; Grebmeier et al., 2006; Woodgate et al., 2005; Figure 1).

AO is a key feature of the Arctic region climate. High AO favors a cyclonic circulation in the Russian Arctic diverting eastward the freshwater delivered by Eurasian rivers off the shelf (Morison et al., 2012). The IR and the KR, with an annual run-off of 61 and 132 km³ year⁻¹, respectively (Gordeev et al., 1996), are important sources of terrigenous material into the ESS (Bröder et al., 2019). To the west, the Lena River (LR), with a water discharge of 588 km³ year⁻¹ represents the largest fresh water volume to the LS and the ESS (Holmes et al., 2011). These freshwater inputs affect processes such as freezing, sea-ice formation, melting and transport of sea ice (Aagaard & Carmack, 1989) and thus the distribution of coastal sea ice (Divine et al., 2004; Haine et al., 2015).

Sea ice in the ESS exhibits strong seasonal and interannual variability (Parkinson et al., 1999; Wang et al., 2019). The ESS is entirely frozen from November to April. In May, sea ice around the northern New Siberian Islands begins melting under the influence of winds. In June, inshore sea ice starts thawing and declining. Open water conditions generally establish earlier in the West than in the East-ESS. Sea ice begins freezing in October at a higher freezing rate in the West-ESS. Summer sea-ice coverage in the Arctic Ocean has been decreasing significantly in the past decades leading to ESS evolving from a largely ice-covered area to an area now largely ice-free (Wang et al., 2019).

Sea-ice motion in ESS is affected by wind patterns generally following the wind direction (Morris et al., 1999). On the shallow Siberian continental shelf, the persistent sea breeze in winter causes the formation of polynya or channels at the boundary between land-fast ice and pack ice (Zhang et al., 2021) such as the Great Siberian Polynya that has long existed between the eastern LS and the New Siberian Islands (Bareiss & Görgen, 2005; Speer et al., 2017; Zonn et al., 2016).

SU ET AL. 2 of 14



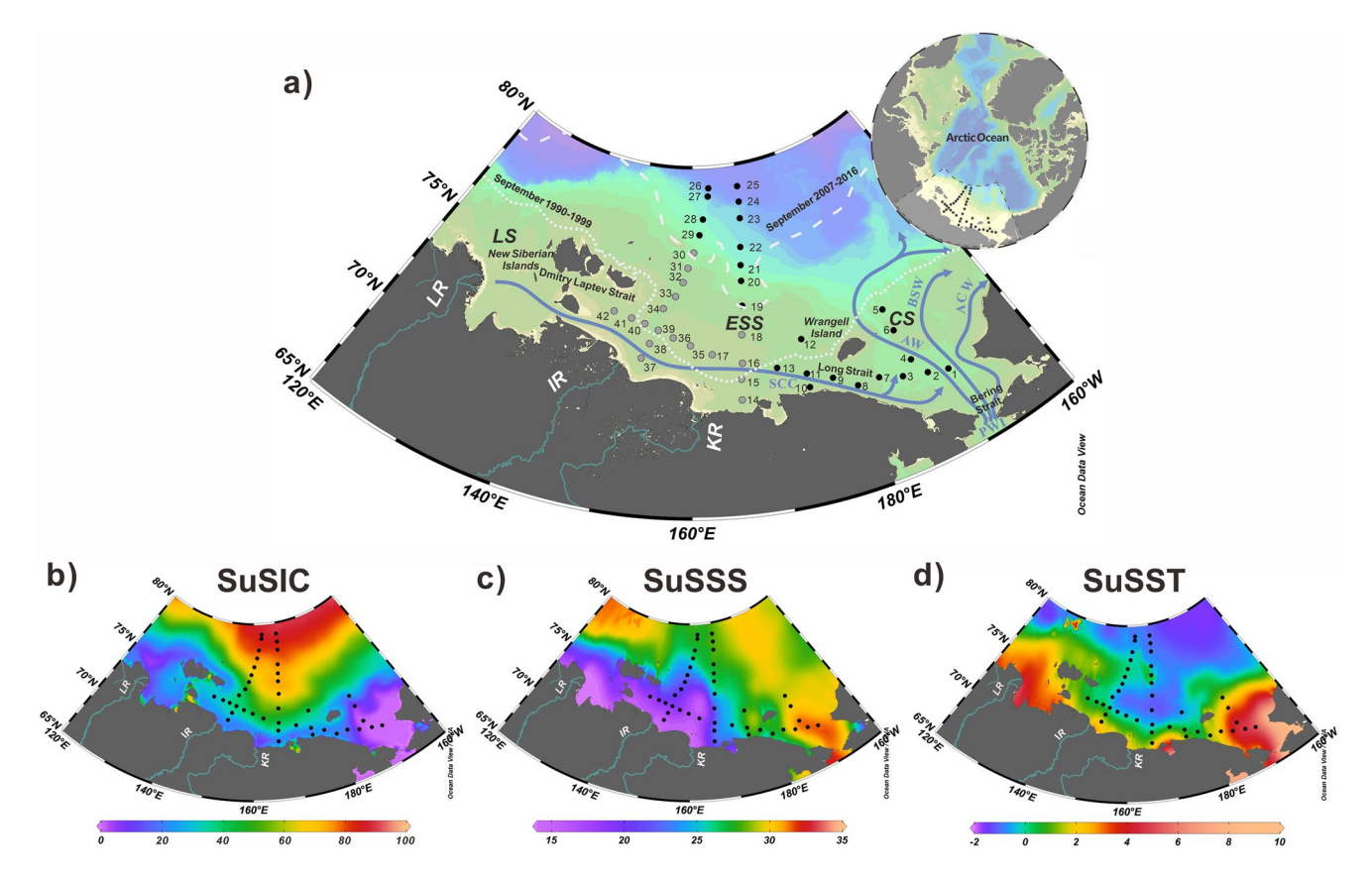


Figure 1. (a) Map of the western Arctic Ocean showing surface ocean circulation (blue arrows) and sampling locations (black dots and gray dots). The stations in gray feature a strong influence of rivers. The black number represents the serial number of the station (see Table S1 in Supporting Information S1 for details). Main study regions: ESS, East Siberian Sea; CS, Chukchi Sea; LS, Laptev Sea (see Figure S1 in Supporting Information S2 for details). The dotted and dashed lines in white represent the 20% isolines of September sea-ice concentration for the period 1990–1999 and 2007–2016, respectively. Typical surface circulation: SCC, Siberian coastal current; PWI, Pacific water inflow (ACW-Alaskan Coastal Water; AW-Anadyr Water; BSW-Bering Shelf Water). Rivers are shown in green lines: LR, Lena River; IR, Indigirka River; KR, Kolyma River. (b) The satellite average Summer Sea-Ice concentration (SuSIC) from 1996 to 2015 obtained from NSIDC (https://nsidc.org). The distribution of mean Summer Sea Surface Salinity (SuSSS) and Summer Sea Surface Temperature (SuSST) from 1955 to 2012 are shown in (c) and (d), respectively. The SuSSS and SuSST data were obtained from Locarnini et al. (2013) and Zweng et al. (2013), respectively.

3. Material and Methods

3.1. Sediment Sampling

A total of 42 surface sediment samples (0–2 cm) were retrieved from the ESS during the Cruise LV77 aboard the R/V *Akademik M.A. Lavrentiev* (Figure 1). The samples were collected using a box-corer and quickly stored at –20°C after recovery. They were freeze-dried prior biomarker analyses in the Key Laboratory of Marine Ecosystem Dynamics, Second Institute of Oceanography, Ministry of Natural Resources (Hangzhou, China).

3.2. Total Organic Carbon (TOC) and Total Nitrogen (TN) Analyses

The TOC and TN were analyzed at the Ocean College, Zhejiang University. For these bulk analyses, samples were also freeze-dried and homogenized. Approximately 1 g of sediment was acidified with 1 mol L^{-1} HCl and left at 50° C for at least 48 hr to remove carbonates. Samples were then washed with ultra-pure water to pH = 7 and then freeze-dried (Williford et al., 2007). Samples were analyzed with an element analyzer (FLASH 2000 CHNS-O, Thermo Fisher) for TOC and TN determination. Reference samples BBOT Thermo were used for quality control. The standard deviation of the measurements is less than <0.1%.

SU ET AL. 3 of 14



3.3. Biomarker Analyses

Lipids were extracted from the freeze-dried sediments using a mixture of dichloromethane/methanol (2:1 v/v) for 10 min in an ultrasonic bath, then centrifuged for 2 min at 2,500 rpm. The supernatant containing the lipids was then retrieved with a clean glass pipette and placed in a clean glass vial. This step was repeated twice, the three extracts were combined and dried under a gentle nitrogen stream. Hydrocarbons, alkenones and sterols were further separated from the total lipid extract using 2.5 ml n-hexane, 4 ml n-hexane/ethyl acetate (90:10 v/v) and 4 ml n-hexane/ethyl acetate (70:30 v/v), respectively, using silica gel as stationary phase (Sicre et al., 2001). After separation, 50 µl BSTFA (bis-trimethylsilyl-trifluoroacetamide) were added to the sterol fraction and heated at 70°C for 1 hr to complete derivatization. Both C₂₅-HBIs (IP₂₅, HBI-II, HBI-III and HBI-IV, a geometric isomer of HBI-III) and sterols were analyzed by gas chromatography (GC, Agilent Technologies 7890) coupled to mass spectrometry (MS, Agilent 262 Technologies 5975C inert XL; Belt et al., 2007; Müller et al., 2011). GC/MS analyses were carried out on a 30 m HP-5MS column (0.25 mm i.d., 0.25 µm film thickness). The oven temperature was programmed from 40°C to 300°C at a heating rate of 10°C min⁻¹ and maintained at final temperature for 10 min. The operating conditions of MS were as follows: ion source temperature at 250°C and ionization energy at 70 eV. Individual compounds were identified based on their retention time with reference compounds and their mass spectra. For quantification of HBIs (m/z 350 for IP₂₅, m/z 348 for HBI-II, and m/z 346 for HBI-III and HBI-IV), 7-hexylnonadecane (m/z 266) was used as an internal standard and added to the sample prior extraction while cholesterol-d6 (cholest-5-en-3β-ol-D6, m/z 464) was used as an external standard and added prior injection to calculate sterol concentrations. The molecular ions m/z 470, m/z 500, m/z 396, and m/z 382 were used to quantify the sterols, brassicasterol (24-methylcholesta-5,22E-dien-3 β -ol), dinosterol (4 α ,23,24R-trimethyl-5 α -cholest-22E-en-3β-ol), 24-ethylcholest-5-en-3-ol and campesterol (24-methylcholest-5-en-3β-ol), respectively. It should be noted that both the α and β isomers of the 24-ethylcholest-5-en-3-ol co-exist in marine sediments. However, the β isomer (24-ethylcholest-5-en-3β-ol) named β-sitosterol of terrigenous origin is found in high abundances in coastal settings except for coastal upwelling areas where the α isomer can prevail due to high productivity (Volkman, 1986). Diatoms can produce β-sitosterol, though in minor amounts, as opposed to cyanobacteria as reported in cyanobacterial mats (Boon et al., 1983). We assume that 24-ethylcholest-5-en-3-ol is primarity β-sitosterol in our samples (see discussion). All concentrations of biomarkers were then normalized to TOC.

3.4. Calculation of the PIP₂₅ Index

Semi-quantitative estimates of sea ice were calculated using the PIP_{25} index that combines sympagic IP_{25} and pelagic phytoplankton biomarker (P) in the following expression (Müller et al., 2011):

$$PIP_{25} = \frac{[IP_{25}]}{[IP_{25}] + [phytoplankton biomarker] * c}$$
 where $c = \frac{mean \ IP_{25} \ concentration}{mean \ phytoplankton biomarker concentration}$

Brassicasterol, dinosterol and HBI-III were used as a reference for pelagic phytoplankton to derive P_BIP_{25} , P_DIP_{25} and $P_{III}IP_{25}$ indexes, respectively. The c value represents the ratio of the mean concentration of IP_{25} over the mean concentration of the selected phytoplankton biomarker of all samples, or the subset after ruling out estuarine samples (salinity <25). Since the abundances of IP_{25} and HBI-III were of similar magnitude in our data set, the $P_{III}IP_{25}$ index was also calculated for c=1.

3.5. Oceanographic Data

The satellite sea-ice concentration (SIC) data were obtained from the Nimbus-7 SMMR and DMSP SSM/I-SS-MIS passive microwave data of the National Snow and Ice Data Center (NSIDC, https://nsidc.org). Here, we selected the average SIC from 1996 to 2015 to generate SIC for spring (Sp; April, May, and June) and summer (Su; July, August, and September) and the 20% isolines of September SIC shown in Figure 1.

Based on the range of sedimentation rate in most of the study area $(1.1-1.6 \text{ mm year}^{-1}; \text{ Bröder et al., } 2016; \text{ Vonk et al., } 2012)$, the top 2 cm of the surface sediments represent between ~20 and ~30 years. During this period, the Arctic sea ice experienced relatively stable icy years in 1990–1999 followed by a decade of significant sea-ice

SU ET AL. 4 of 14

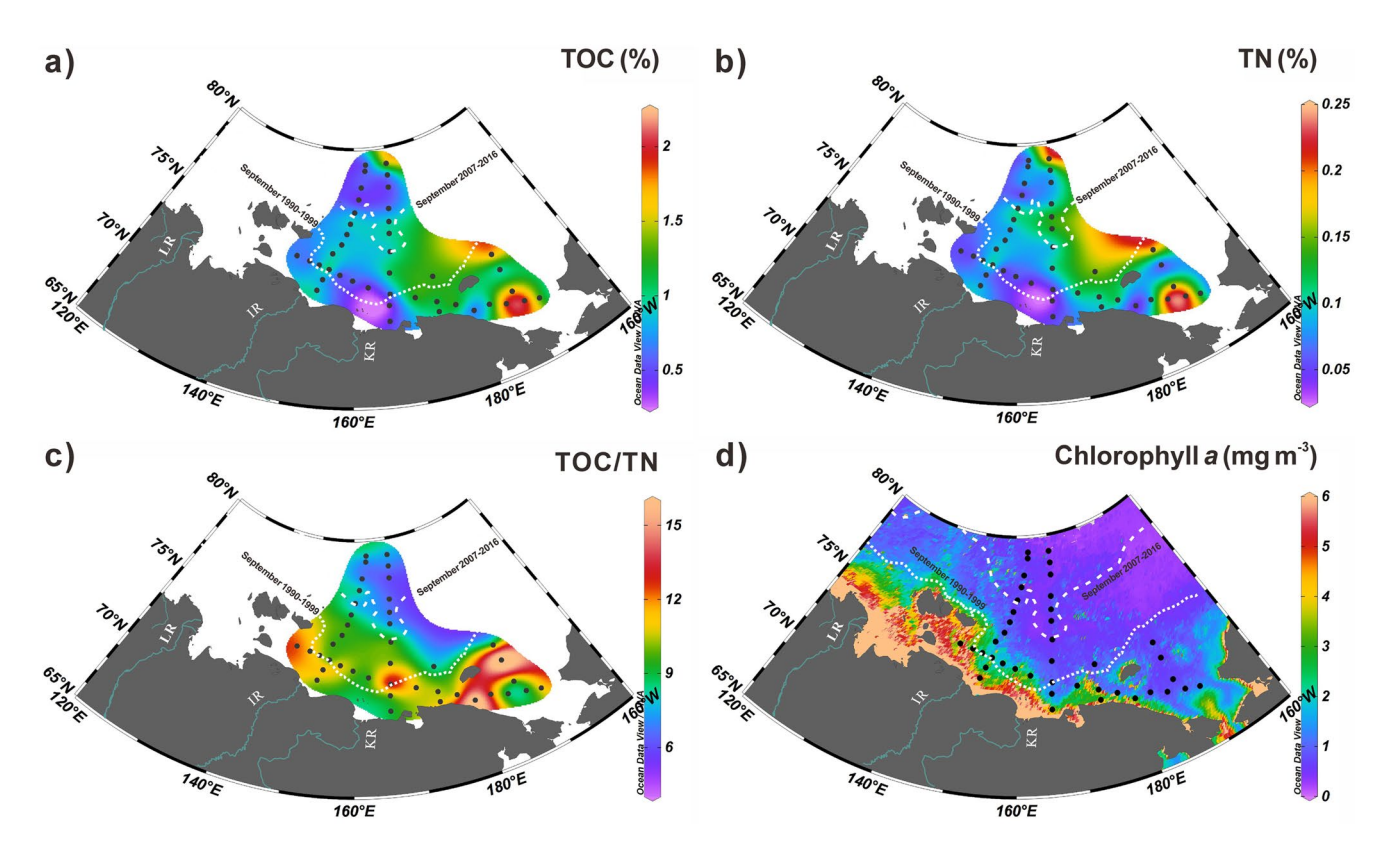


Figure 2. Distribution of (a) TOC, (b) TN and (c) TOC/TN in the surface sediments of ESS and CS. (d) Map showing the average chlorophyll *a* in May-September (1998–2016) in the ESS (GlobColour, https://hermes.acri.fr/). Isolines of September 20% sea-ice concentration for the period 1990–1999 and 2007–2016 are presented in white dotted and dashed lines, respectively (NSIDC, https://nsidc.org).

retreat in 2007–2016 (NSIDC, https://nsidc.org). These two situations are shown in Figure 1 by the average summer minimum sea ice (20% of SIC) from 1990 to 1999 and from 2007 to 2016, respectively.

The chlorophyll *a* data were obtained from the Moderate Resolution Imaging Spectroradiometer (MODIS) on the Aqua satellite, using the GlobColour processing results (https://hermes.acri.fr/). The May to September mean value of chlorophyll *a* from 1998 to 2016 was used. Summer sea surface salinity (SuSSS) and temperature (SuSST) data are from World Ocean Atlas 2013 (WOA13, https://www.nodc.noaa.gov/OC5/woa13/) with 0.25° grid. A map showing the different regions and their acronyms used in the discussion is provided in Figure S1 in Supporting Information S2.

4. Results

4.1. Total Organic Carbon (TOC) and Total Nitrogen (TN)

The values of TOC and TN in the ESS span from 0.2% to 2.1% and from 0.03% to 0.22%, respectively (Figures 2a and 2b; Table S1 in Supporting Information S1). Maximum TOC values of 1.7%–2.1% are found in the East-ESS/West-CS, while lowest ones (<0.5%) occur off the KR mouth and highest latitudes. The spatial distribution of TN values shares strong resemblance with TOC (Table S1 in Supporting Information S1).

4.2. Sterols

Brassicasterol shows high values in the central ESS (141–191 μg g⁻¹ TOC, Table S1 in Supporting Information S1, Figure 3a), while dinosterol is generally low across the basin except for high values east of Wrangel Island under the influence of AW (9–14 μg g⁻¹ TOC; Table S1 in Supporting Information S1, Figure 3b). Terrestrial campesterol and β -sitosterol both show extremely low values in the northernmost area as for brassicasterol

SU ET AL. 5 of 14

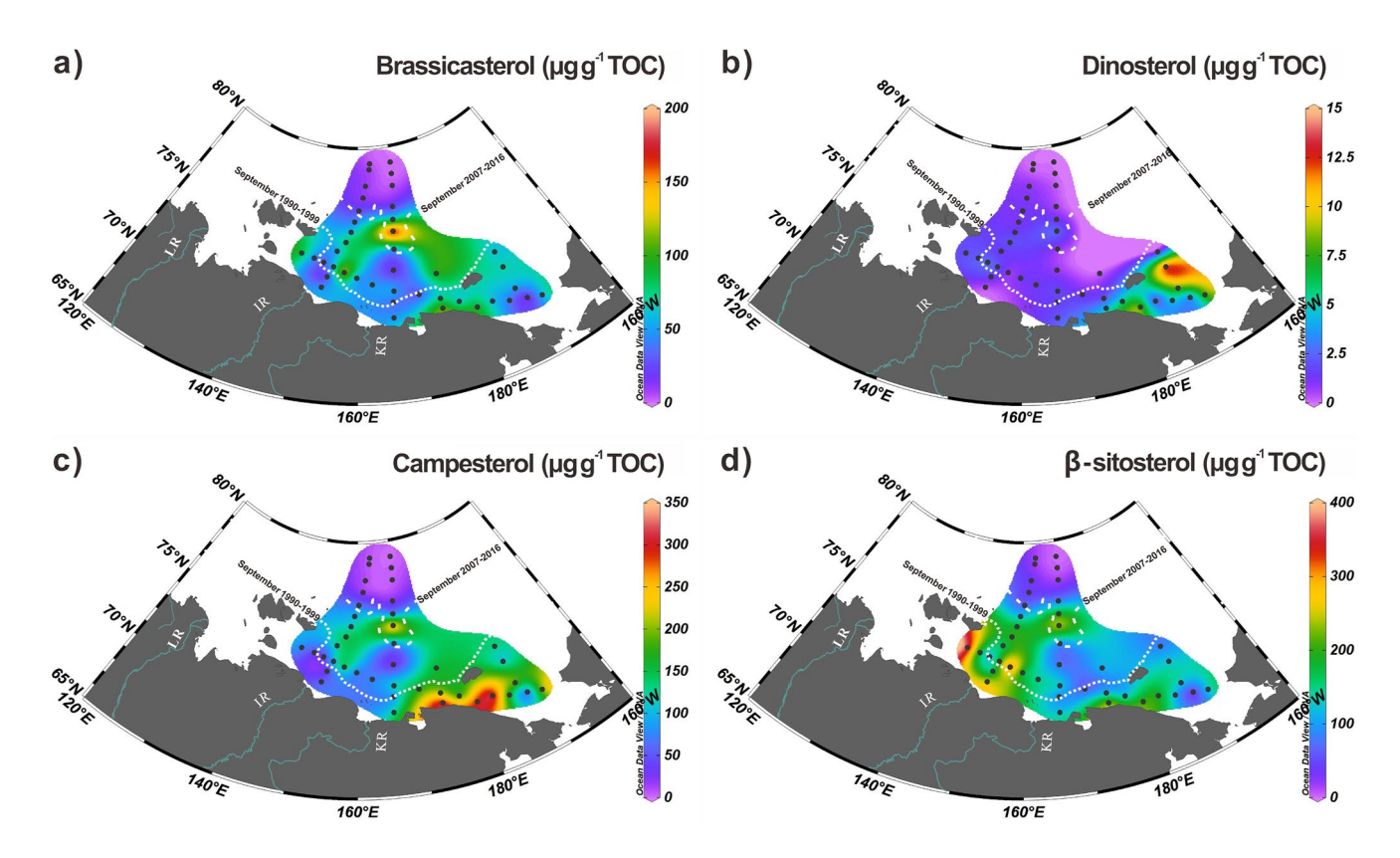


Figure 3. Concentrations (μg g^{-1} TOC) of phytoplankton biomarkers: (a) brassicasterol and (b) dinosterol; terrigenous biomarkers: (c) campesterol and (d) β-sitosterol in the surface sediments of ESS and CS. Isolines of September 20% sea-ice concentration of for the period 1990–1999 and 2007–2016 are presented in white dotted and dashed lines, respectively (NSIDC, https://nsidc.org).

and dinosterol. However, campesterol and β -sitosterol strongly differ along the shelf suggesting different sources (Figures 3c and 3d).

4.3. C₂₅ Highly Branched Isoprenoid (HBI) Alkenes

The distribution patterns of sympagic IP $_{25}$ and HBI-II are generally similar, with high values in the central ESS and near the New Siberian Islands (IP $_{25}$: 1.7–2.4 μg g $^{-1}$ TOC; HBI-II: 1.7–2.7 μg g $^{-1}$ TOC, Table S1 in Supporting Information S1 and Figures 4a and 4b). Values decrease from the central region to nearshore sediments (IP $_{25}$: 0.2–0.7 μg g $^{-1}$ TOC; HBI-II: 0.1–0.4 μg g $^{-1}$ TOC, Table S1 in Supporting Information S1) and reach a minimum at high latitudes (IP $_{25}$: 0.06–0.4 μg g $^{-1}$ TOC; HBI-II: 0.08–0.5 μg g $^{-1}$ TOC, Table S1 in Supporting Information S1). IP $_{25}$ and HBI-II are also low in the West-CS.

HBI-III and HBI-IV show very similar patterns with a maximum south and east of Wrangel Island that strikingly contrast with the sympagic HBIs (0.11–1.68 μg g⁻¹ TOC; Figures 4a and 4b). Intermediate values occur in the central ESS (1.8–2.7 μg g⁻¹ TOC) while lowest ones are found in coastal waters and at highest latitudes (Figures 4c and 4d). The HBI-IV sediment content is generally <2 μg g⁻¹ TOC (Figures 4c and 4d, Table S1 in Supporting Information S1) except for south and east Wrangel Island (Figures 4c and 4d, 6.8–8.5 μg g⁻¹ TOC, Table S1 in Supporting Information S1), as also found for HBI-III.

5. Discussion

5.1. Organic Carbon Sources

TOC in the ESS coastal surface sediments results from mixed inputs of marine primary production and terrigenous sources (Vonk et al., 2012). *n*-Alkanes in sediments indicate a gradually decrease of terrestrial organic carbon from south to north, along a transect from the IR estuary to offshore (Petrova et al., 2004). Similar trends

SU ET AL. 6 of 14

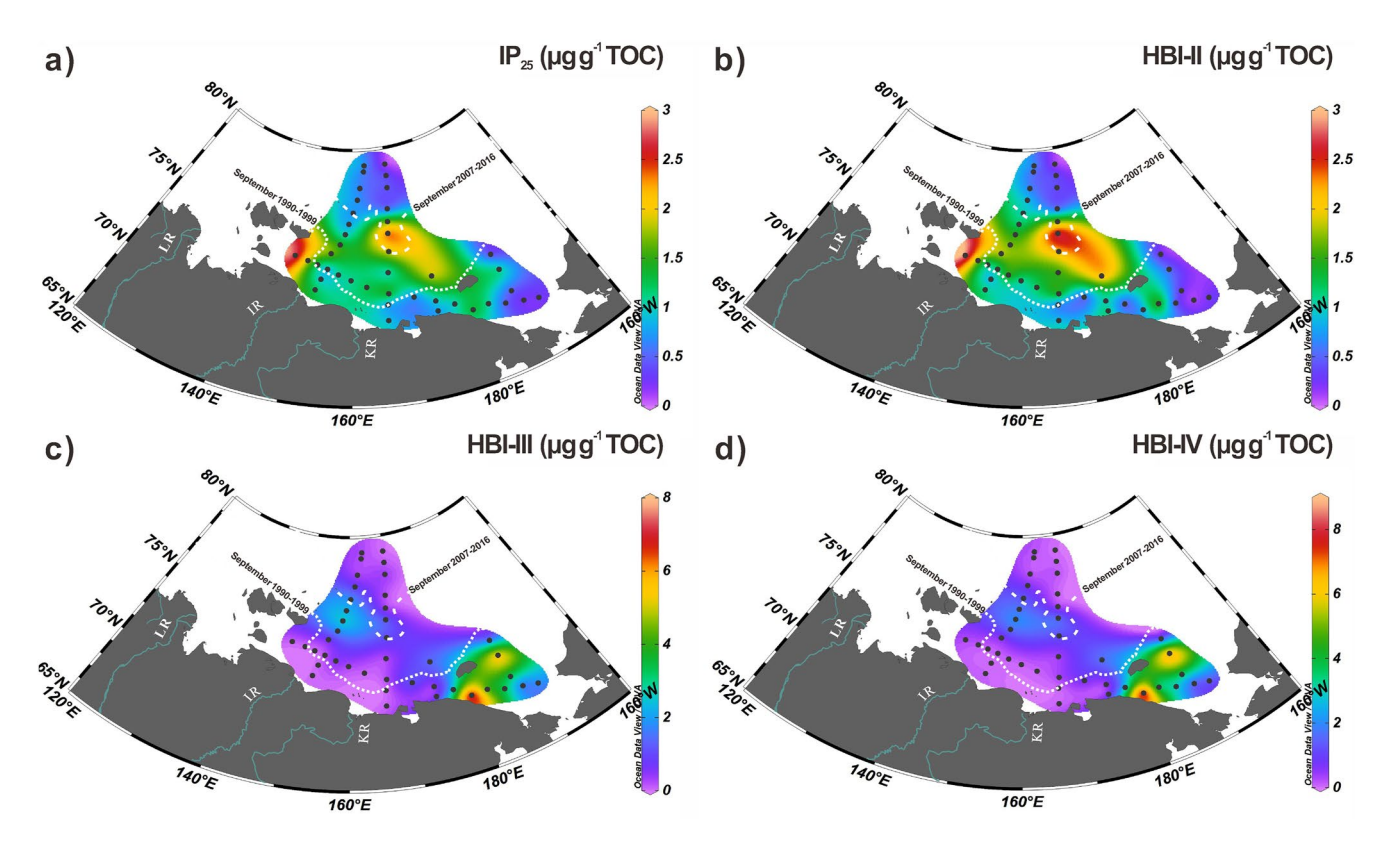


Figure 4. Concentrations (μg g⁻¹ TOC) of HBIs: (a) IP₂₅, (b) HBI-II, (c) HBI-III, and (d) HBI-IV in surface sediments. Isolines of September 20% sea-ice concentrations for the period 1990–1999 and 2007–2016 are presented in white dotted and dashed lines, respectively (NSIDC, https://nsidc.org).

are observed in the C/N ratios (Figure 2c) and terrestrial sterols (Figure 3). In the outer East-ESS and West Wrangle Island, the prevailing source of TOC is generally marine as indicated by C/N ratio <8 (Figure 2c), high dinosterol (>5 μ g g⁻¹ TOC, Figure 3b) and brassicasterol concentrations (>100 μ g g⁻¹ TOC, Figure 3a). This result is consistent with warm and nutrient-rich PWI flowing into the CS through the Bering Strait sustaining high primary production and export in the East-ESS and West-CS, leading to organic rich sediments till around 170°E (Figure 2a; Bröder et al., 2019; Sparkes et al., 2016; Stein & Macdonald, 2004; Tesi et al., 2014).

In the nearshore West-ESS sediments, high C/N ratio >10 and β -sitosterol concentrations (>200 μg g⁻¹ TOC) highlight strong imprint of terrigenous material (Figures 2c and 3d). Marginal seas such as the Kara and Laptev Seas are also strongly affected by land run-off and nearshore area (Fernandes & Sicre, 2000; Peulvé et al., 1996) as indicated by high C/N ratio and n-alkanes ($C_{27} + C_{29} + C_{31}$; Stein & Fahl, 2004a, 2004b). This is also in agreement with previous reports of lower δ^{13} C of TOC values ($-27.4\%c \sim -25.5\%c$; Bröder et al., 2019) and high lignin concentrations (0.9–1.2 mg g⁻¹ TOC; Salvadó et al., 2016) in the ESS.

In areas of significant amount of seasonal sea ice (73°-76°N), high TOC is generally associated with enhanced primary production as reflected by concomitant high TN. At highest latitudes, North of 77°N, the low TOC sediment content reflects minor terrigenous organic carbon and limited primary production and export due to permanent sea ice. The distribution of spring and summer chlorophyll *a* in surface waters suggest enhanced primary production in the coastal waters of the ESS (Figure 2d). However, higher brassicasterol levels are found in the central ESS rather than in the coastal areas reflecting enhanced marine production in the marginal ice zone (MIZ; Figure 3a). This mismatch between phytosterol and chlorophyll patterns can in part be explained by the known bias of optically complex (Case 2) waters induced by high suspended particle load of more turbid coastal waters leading to the overestimation of chlorophyll *a* concentrations. Terrestrial colored dissolved organic matter (CDOM) is another source of bias of chlorophyll *a* concentrations caused by the abnormally high absorption of CDOM at low phytoplankton biomass such as in shelf waters (Lewis & Arrigo, 2020). Overall, primary production in the ESS is strongly affected by terrigenous suspended particles delivered in nearshore waters. Highly

SU ET AL. 7 of 14



turbid waters together with fluctuating salinity likely explain brassicasterol minima off the IR and KR river mouths, a result that can introduce complication in the interpretation of sea-ice proxy indexes using sterols.

5.2. Phytoplankton Biomarkers

Brassicasterol is primarily produced by marine diatoms thriving in open sea waters or at the sea-ice edge, while dinosterol is commonly synthesized by dinoflagellates in open sea waters (Volkman, 1986). In contrast to the Kara and Laptev Seas (Xiao et al., 2013), these two phytosterols do not show similar distributions in the ESS (Figures 3a and 3b). No clear correlation between IP₂₅ and brassicasterol was found by Xiao, Fahl, et al. (2015) and Kolling et al. (2020). In addition, in our study the distribution pattern of brassicasterol seems to match with that of IP₂₅ and HBI-II while dinosterol shares stronger resemblance with HBI-III and HBI-IV (Figures 2a, 2b and 3). These findings agree with brassicasterol production being associated with nutrient-rich conditions of the sea-ice edge while turbid waters off the IR and KR deltas do not provide favorable conditions to marine diatom growth. Therefore, different local and regional phytoplankton source and distribution are expected from different drainage basin, water discharge and suspended load of Eurasian rivers (Kolling et al., 2020; Xiao, Fahl, et al., 2015). Although dinosterol is also affected by estuarine conditions, its concentration remain relatively homogeneous across the ESS. It is noteworthy that this sterol in our samples is an order of magnitude lower than found by Stoynova et al. (2013) by using different extraction methods and internal standard quantification.

HBI-III is produced by diatoms living at the sea-ice edge and in ice-free waters (Bai et al., 2019; Belt, 2018; Smik, Cabedo-Sanz, & Belt, 2016). A one-year sediment trap time series from the CS has consistently shown higher production of HBI-III at low sea-ice concentrations (Bai et al., 2019). This finding is in line with low to moderate values of HBI-III (and HBI-IV) in the central to East-ESS, between the two isolines of September minimum ice edge (Figure 4c) and previous interpretation of HBI-III distribution (Arrigo et al., 2014; Collins et al., 2013; Smik, Belt, et al., 2016). Highest HBI-III and HBI-IV are likely reflecting the earlier retreat of sea ice in the West-CS than in the ESS and the inflow of nutrient-rich PWI providing favorable conditions for their production. By contrast, HBI-III and HBI-IV concentrations are extremely low in nearshore and coastal waters as opposed to sympagic HBIs that show moderate levels. Only in the permanent sea-ice area, do all HBIs show low levels. In summary, HBI-III and HBI-IV as well as dinosterol were low or absent in the permanent sea ice and nearshore waters while enhanced in West-CS. Intermediate values were found in the MIZ where brassicasterol and sympagic HBIs were abundant in accordance with our present knowledge on these biomarkers. HBI-III production is thus consistent with open water conditions (Belt, 2018, 2019; Köseoğlu et al., 2018; Smik, Cabedo-Sanz, & Belt, 2016) although recently Amiraux et al. (2021) reported the occurrence of this HBI in sea ice in southwest Baffin Bay.

5.3. IP₂₅ Variability and Spring/Summer Sea-Ice Condition

 IP_{25} is found throughout the ESS (Figure 4a). The distribution patterns of IP_{25} and HBI-II are generally similar (Belt et al., 2016) as reported in earlier studies in the Arctic Ocean (Koch et al., 2020; Xiao, Fahl, et al., 2015) as opposed to Baffin Bay (Kolling et al., 2020). At high latitudes (North of 77°N), lowest IP_{25} together with lowest phytosterols and other HBIs are consistent with permanent sea ice. In the outer continental shelf, melting does not take place until the end of summer resulting in an extremely short phytoplankton growing season. In the eastern New Siberian Islands maximum IP_{25} can be explained by favorable production conditions. Indeed, longest season of fast ice formation has been observed between the New Siberian Islands and the coast (Yu et al., 2014). In addition, wind-driven polynya formation and channels between land-fast ice and pack ice also cause sea-ice diatom blooms (Zhang et al., 2021).

In the central ESS, simultaneous high concentrations of IP_{25} , HBI-II and brassicasterol and moderate HBI-III concentrations underpin MIZ conditions (Figures 3a and 4a–4c). Similarly, maximum abundance of IP_{25} during summer is consistent with sediment trap data under MIZ conditions characterized by sea-ice algae production throughout the Arctic Ocean (Bai et al., 2019; Fahl & Stein, 2012; Koch et al., 2020; Nöthig et al., 2020). We can thus conclude that seasonal sea-ice edge and/or MIZ conditions prevailed in the central ESS over the last decades.

Lower IP_{25} values in the nearshore are expected from North-South sea-ice cover trends across the ESS in spring/summer. Xiao, Fahl, et al. (2015) also found low IP_{25} production in the LS due to freshening by riverine waters. Other factors such as water turbidity in the river plume, erosion and sediment resuspension in shallow waters

SU ET AL. 8 of 14



| Table 1 |
|---|
| Comparison of Coefficient of Determination (r ²) for Correlations Between PIPs and Sea-Ice Concentrations in Summer |
| (SuSIC) and Spring (SpSIC) |

| | Estuarine samples included $(n = 42)$ | | Estuarine samples excluded $(n = 24)$ | |
|-----------------------------|---------------------------------------|-------|---------------------------------------|-------------|
| | SpSIC | SuSIC | SpSIC | SuSIC |
| IP ₂₅ | 0.09 | <0.01 | 0.11 | 0.01 |
| $P_{III}IP_{25} (c \neq 1)$ | 0.23 | 0.12 | 0.47 | 0.73 |
| $P_{III}IP_{25} (c=1)$ | 0.22 | 0.11 | 0.42 | <u>0.70</u> |
| P_BIP_{25} | 0.19 | 0.41 | 0.27 | 0.58 |
| P_DIP_{25} | 0.51 | 0.46 | 0.65 | 0.66 |

Note. All p < 0.01; Data bold and underlined indicate significant correlation.

caused by upwelling along the coast all concur to reduce phytoplankton production (Osadchiev, Silvestrova, et al., 2020; Osadchiev, Pisareva, et al., 2020). Lowest sympagic HBIs in West-CS are coherent with the early sea-ice retreat caused by summer SSTs reflecting the influence of the PWI. In general, we found a very weak correlation between IP₂₅ and spring or summer SIC (SpSIC: $r^2 = 0.09$, p < 0.01; SuSIC: $r^2 < 0.01$, p < 0.01; Table 1).

5.4. PIP₂₅ Indexes

At latitudes North of 77°N, all PIP_{25} values were >0.75 (Figures 5a–5c; Figure S2 in Supporting Information S2) reflecting permanent sea-ice cover. IP_{25} and phytoplankton biomarkers show intermediate to high concentration values in areas lying between the summer 20% SIC isoline of 1990–1999 (time interval of stable icy conditions) and that of 2007–2016 (time interval when sea-ice extent decreased rapidly; Figures 3 and 4). In this area, PIP_{25} values are comprised between 0.4 and 0.7 reflecting the gradual northward retreat of sea ice providing optimum

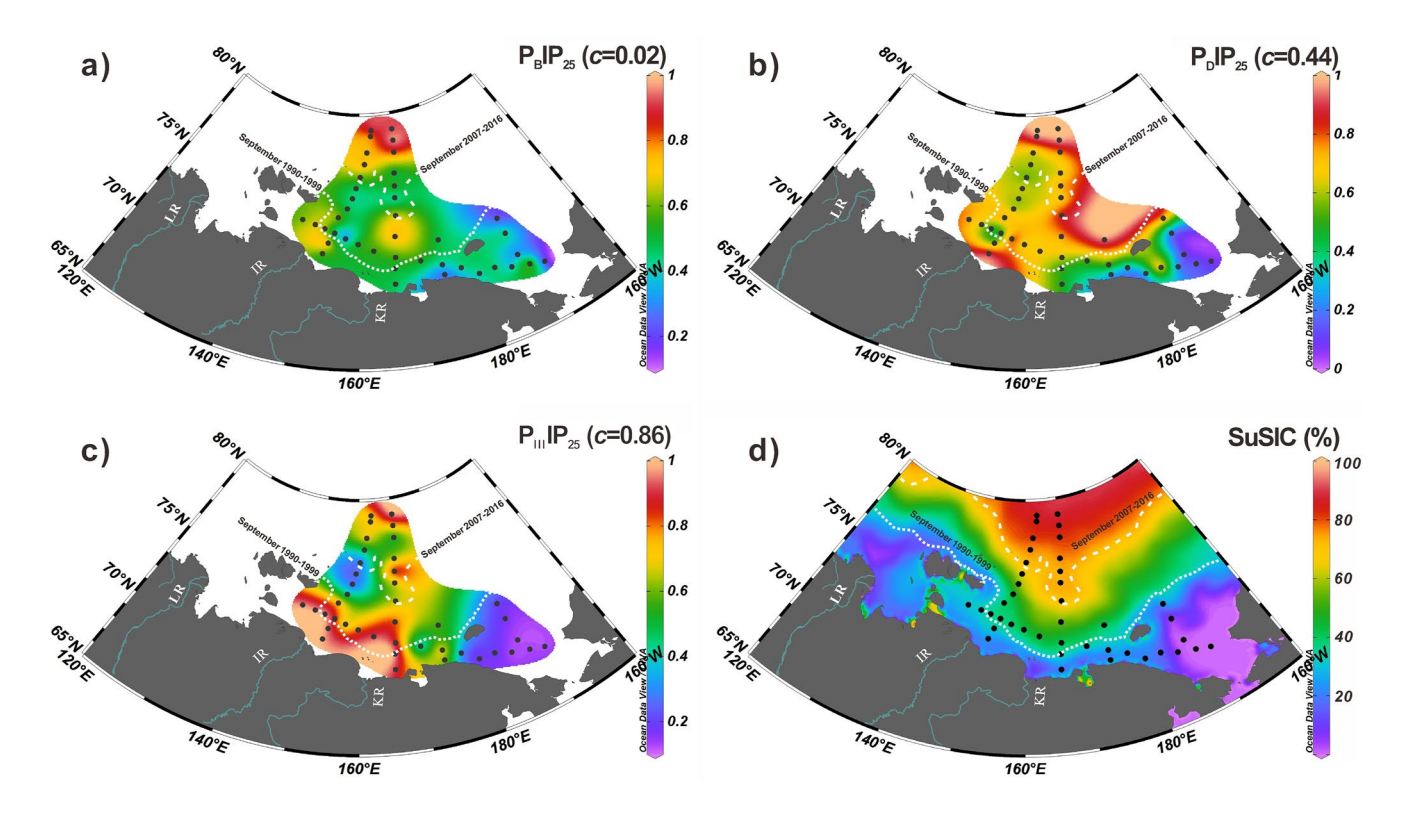


Figure 5. Distribution of PIP_{25} and the satellite SuSIC: (a) P_BIP_{25} based on brassicasterol; (b) P_DIP_{25} based on dinosterol; (c) $P_{III}IP_{25}$ based on HBI-III; (d) the satellite average SuSIC from 1996 to 2015 were obtained from NSIDC (https://nsidc.org). September sea-ice concentration of 20% for the period 1990–1999 and 2007–2016 are presented in white dotted and dashed lines, respectively (NSIDC, https://nsidc.org).

SU ET AL. 9 of 14

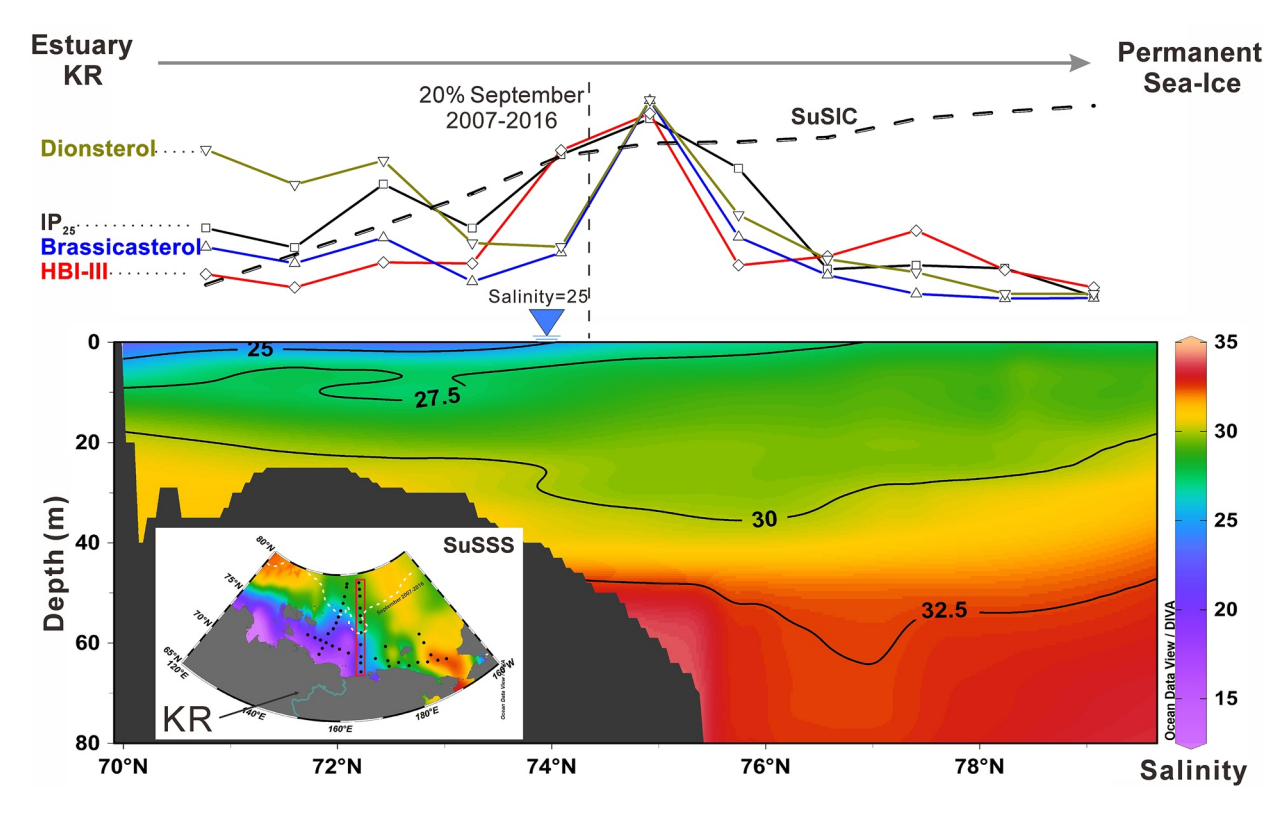


Figure 6. Biomarker distribution along 166°E corresponding transect from off the KR estuary to permanent sea ice. The upper panel shows the concentrations of HBIs and sterols. The transect of SuSIC is obtained from the satellite average SuSIC from 1996 to 2015 (NSIDC, https://nsidc.org). The lower panel displays the summer salinity of the upper 80 m water depths with isohalines (1955–2012, Zweng et al., 2013). The salinity front between the riverine discharge and open ocean is marked by salinity = 25. The inset map indicates the transect with the SuSSS distribution (more detailed information can be found in Figure 1).

living conditions for sea-ice diatoms and phytoplankton growth in agreement with previous observations in the CS (Hill et al., 2018).

P_{III}IP₂₅ and P_DIP₂₅ in the West-CS depict broadly similar distribution with values <0.2 indicating low sea ice to open water conditions and high phytoplankton production. At nearshore sites of the ESS, owing to the influence of fresh water and terrigenous inputs from the IR and KR, the production and export of biomarkers differ from those of open ocean waters. Surface salinity is another factor that may affect phytoplankton distribution as shown in Figure 6 by the abundances of IP25, HBI-III, brassicasterol and dinosterol along the 166°E meridian (from Zweng et al., 2013) and thus bias PIP₂₅. For instance, low or undetectable HBI-III led to abnormally high P_{III}IP₂₅ values (Figures 4c and 5c) that are close to those of permanent sea ice (Figure 5d). This result underscores unfavorable conditions for pelagic phytoplankton to prosper such as stratification and enhanced turbidity of Eurasian rivers plumes spreading and mixing with the narrow SCC over the shelf. Biases are also evident from intermediate values of P_BIP₂₅ off the IR mouth resulting in misleading estimates of high seasonal SIC. However, dinosterol remains rather high over the shelf suggesting possible adaptation of dinosterol producers (dinoflagellates) to variable salinity and suspended load (Kraberg et al., 2013; Nelson & Sachs, 2014; Wu et al., 2020). Interestingly, PDIP25 values are low at sites influenced by IR and KR run-off except for one site near the IR mouth (Figure 5b). In the LR estuary, however, the concentrations of dinosterol remain low compared to those of brassicasterol possibly reflecting freshwater producers of the latter (Figure S3 in Supporting Information S2; Xiao, Fahl, et al., 2015). Such departures should be carefully considered when using PIP₂₅ index to reconstruct paleo-sea-ice in deltaic settings (Belt, 2018; Kolling et al., 2020; Xiao, Fahl, et al., 2015).

Weak correlations were found between PIP₂₅ and SIC (either SpSIC or SuSIC, $r^2 < 0.41$, p < 0.01), except for P_DIP₂₅ (Tables 1, Table S2 in Supporting Information S1; n = 42, $r^2 = 0.51$, p < 0.01). However, our set of surface sediments encompasses a range of deposition rates. In addition, from coastal waters to open sea, the ESS covers variable environmental and sea-ice conditions (Petrova et al., 2004; Stein, 2008). The deposition rate over

SU ET AL. 10 of 14



the continental shelf is about 1.1-1.6 mm year⁻¹ (Bröder et al., 2016; Vonk et al., 2012) and decreases to 0.09-0.02 mm year⁻¹ toward the deep-sea basin (Li et al., 2020; Stein & Fahl, 2000). Owing to different deposition rates within our sites, the top 2 cm of sediment may represent different time interval, which can account in part for the departure from linear relationship between PIP_{25} and SIC. Of course, the source uncertainty of brassicasterol in coastal waters also reduced the correlation between P_BIP_{25} and SuSIC (Volkman, 1986). The relationship is improved after removal of sites with salinity less than 25 (summer salinity gradient between the estuary and open ocean, from World Ocean Atlas 2013 by Zweng et al., 2013; Table 1, Table S3 in Supporting Information S1, and Figure S4 in Supporting Information S2). Overall, our findings suggest that P_DIP_{25} might be more suitable for sea-ice reconstruction in coastal waters influenced by river run-off (Table 1). High concentrations of terrestrial sterols (campesterol and β -sitosterol) have been found in the Siberian marginal sea estuaries (Figures 3c and 3d; Xiao et al., 2013, 2015), implying them as proxies for riverine input. Therefore, terrestrial sterols (or other terrestrial proxies) should be considered when using IP_{25}/PIP_{25} to reconstruct paleo-sea-ice environment to discern the influence of continental run-off.

6. Conclusions

Spatial mapping of sympagic HBIs and pelagic phytoplankton biomarkers from 42 surface sediments revealed differences across the ESS and the West-CS. High productivity was inferred from dinosterol, HBI-III and HBI-IV concentrations in West-CS sediments as a result of the nutrient-rich PWI and early retreat of sea ice allowing for a longer algal production season. Low marine production characterized nearshore sites of the ESS most likely due to Eurasian River plumes and their eastward propagation along with the SCC. Stratification induced by freshwater from the IR and KR rivers combined with high suspended load likely account for reduced primary production in the ESS shelf waters.

Highest concentrations of IP₂₅, brassicasterol, dinosterol and HBI-III found around 74°N, coincide with the average summer ice edge (20% SIC isoline) for the 2007–2016 interval, reflecting the average MIZ conditions. IP₂₅ and PIP₂₅ indexes in the ESS did not show significant correlations with SpSIC or SuSIC except for P_DIP_{25} . This result suggests that dinosterol production was less affected by riverine inputs. Noteworthy, the generally low values of phytoplankton biomarkers in nearshore sediments at comparable levels as those found in permanent sea-ice areas at high latitudes underscore the potential PIP₂₅ biases and subsequently erroneous SIC estimates. Our study overall warns cautiously about the use of PIP₂₅ in regions where continental run-off is significant.

Conflict of Interest

The authors declare no conflicts of interest relevant to this study.

Data Availability Statement

All data in this study are presented in supporting information files and are available under (https://doi.org/10.1594/PANGAEA.934576).

References

Aagaard, K., & Carmack, E. C. (1989). The role of sea ice and other fresh water in the Arctic circulation. *Journal of Geophysical Research*, 94(C10), 14485–14498. https://doi.org/10.1029/JC094iC10p14485

Amiraux, R., Archambault, P., Moriceau, B., Lemire, M., Babin, M., Memery, L., et al. (2021). Efficiency of sympagic-benthic coupling revealed by analyses of n-3 fatty acids, IP₂₅ and other highly branched isoprenoids in two filter-feeding Arctic benthic molluscs: *Mya truncata* and *Serripes groenlandicus*. *Organic Geochemistry*, 151, 104160. https://doi.org/10.1016/j.orggeochem.2020.104160

Arrigo, K. R. (2014). Sea ice ecosystems. Annual Review of Marine Science, 6, 439–467. https://doi.org/10.1146/annurev-marine-010213-135103
Arrigo, K. R., Perovich, D. K., Pickart, R. S., Brown, Z. W., van Dijken, G. L., Lowry, K. E., et al. (2014). Phytoplankton blooms beneath the sea ice in the Chukchi Sea. Deep Sea Research Part II: Topical Studies in Oceanography, 105, 1–16. https://doi.org/10.1016/j.dsr2.2014.03.018
Bai, Y., Sicre, M.-A., Chen, J., Klein, V., Jin, H., Ren, J., et al. (2019). Seasonal and spatial variability of sea ice and phytoplankton biomarker flux in the Chukchi Sea (western Arctic Ocean). Progress in Oceanography, 171, 22–37. https://doi.org/10.1016/j.pocean.2018.12.002

Bareiss, J., & Görgen, K. (2005). Spatial and temporal variability of sea ice in the Laptev Sea: Analyses and review of satellite passive-microwave data and model results, 1979 to 2002. Global and Planetary Change, 48(1–3), 28–54. https://doi.org/10.1016/j.gloplacha.2004.12.004

Belt, S. T. (2018). Source-specific biomarkers as proxies for Arctic and Antarctic sea ice. *Organic Geochemistry*, 125, 277–298. https://doi.org/10.1016/j.orggeochem.2018.10.002

Acknowledgments

We acknowledge the crew and the Russian-Chinese scientific party of R/V Akademik M.A. Layrentiev for their professional sampling work. We are indebted to Jiaqi Wu of Second Institute of Oceanography for her helpful advice and to Prof. Hao Zheng and Yiwen Pan of Zhejiang University for their kind help in the TOC measurement. Vincent Klein of Sorbonne Université is also thanked for technical assistance. This study is financially supported by the National Natural Science Foundation of China (Nos. 41606052, 41941013, 41976229, 42076242), the National Key Research and Development Program of China (No. 2019YFC1509101). the Marine S&T Fund of Shandong Province for Pilot National Laboratory for Marine Science and Technology (Qingdao; No. 2018SDKJ0104-3), the Scientific Research Funds of the Second Institute of Oceanography, State Oceanic Administration, China (Nos. JG1611, JG1911, JG1806) and the Russian Science Foundation (Grant 21-17-00081). M.-A. Sicre thanks the Centre National de la Recherche Scientifique (CNRS) for salary support. We are grateful to Rüdiger Stein and two anonymous reviewers who provided useful suggestions for the manuscript improvement.

SU ET AL. 11 of 14



- Belt, S. T. (2019). What do IP₂₅ and related biomarkers really reveal about sea ice change? *Quaternary Science Reviews*, 204, 216–219. https://doi.org/10.1016/j.quascirev.2018.11.025
- Belt, S. T., Massé, G., Rowland, S. J., Poulin, M., Michel, C., & LeBlanc, B. (2007). A novel chemical fossil of palaeo sea ice: IP25. *Organic Geochemistry*, 38, 16–27. https://doi.org/10.1016/j.orggeochem.2006.09.013
- Belt, S. T., & Müller, J. (2013). The Arctic sea ice biomarker IP₂₅: A review of current understanding, recommendations for future research and applications in palaeo sea ice reconstructions. *Quaternary Science Reviews*, 79, 9–25. https://doi.org/10.1016/j.quascirev.2012.12.001
- Belt, S. T., Smik, L., Brown, T. A., Kim, J. H., Rowland, S. J., Allen, C. S., et al. (2016). Source identification and distribution reveals the potential of the geochemical Antarctic sea ice proxy IPSO25. *Nature Communications*, 7, 12655. https://doi.org/10.1038/ncomms12655
- Boon, J. J., Hines, H., Burlingame, A. L., Klok, J., Rijpstra, W. C., Leeuw, J. W. D., et al. (1983). Organic geochemical studies of Solar Lake laminated cyanobacterial mats. In Bjoroy, M., et al. (Eds.), Advances in organic geochemistry 1981 (pp. 239–248). Wiley.
- Bröder, L., Andersson, A., Tesi, T., Semiletov, I., & Gustafsson, Ö. (2019). Quantifying degradative loss of terrigenous organic carbon in surface sediments across the Laptev and East Siberian Sea. Global Biogeochemical Cycles, 33, 85–99. https://doi.org/10.1029/2018GB005967
- Bröder, L., Tesi, T., Andersson, A., Eglinton, T. I., Semiletov, I. P., Dudarev, O. V., et al. (2016). Historical records of organic matter supply and degradation status in the East Siberian Sea. *Organic Geochemistry*, 91, 16–30. https://doi.org/10.1016/j.orggeochem.2015.10.008
- Brown, T. A., Belt, S. T., Tatarek, A., & Mundy, C. J. (2014). Source identification of the Arctic sea ice proxy IP₂₅. *Nature Communications*, 5, 4197. https://doi.org/10.1038/ncomms5197
- Cai, W.-J., Chen, L., Chen, B., Gao, Z., Lee, S. H., Chen, J., et al. (2010). Decrease in the CO₂ uptake capacity in an ice-free Arctic Ocean basin.
- Science, 329(5991), 556–559. https://doi.org/10.1126/science.1189338
 Cavalieri, D. J., Gloersen, P., Parkinson, C. L., Comiso, J. C., & Zwally, H. J. (1997). Observed hemispheric asymmetry in global sea ice changes.
- Science, 278(5340), 1104–1106. https://doi.org/10.1126/science.278.5340.1104

 Coachman, L. K., & Aagaard, K. (1966). On the water exchange through Bering Strait. Limnology & Oceanography, 11, 44–59. https://doi.
- org/10.4319/lo.1966.11.1.0044
 Collins, L. G., Allen, C. S., Pike, J., Hodgson, D. A., Weckström, K., & Massé, G. (2013). Evaluating highly branched isoprenoid (HBI) biomark-
- ers as a novel Antarctic sea-ice proxy in deep ocean glacial age sediments. *Quaternary Science Reviews*, 79, 87–98. https://doi.org/10.1016/j. quascirev.2013.02.004
- Comiso, J. C. (2012). Large decadal decline of the Arctic multiyear ice cover. Journal of Climate, 25(4), 1176–1193. https://doi.org/10.1175/ JCLI-D-11-00113.1
- Cronin, T. M., Polyak, L., Reed, D., Kandiano, E. S., Marzen, R., & Council, E. (2013). A 600-ka Arctic sea-ice record from Mendeleev Ridge based on ostracodes. *Quaternary Science Reviews*, 79, 157–167. https://doi.org/10.1016/j.quascirev.2012.12.010
- de Vernal, A., Radi, T., Zaragosi, S., Van Nieuwenhove, N., Rochon, A., Allan, E., et al. (2020). Distribution of common modern dinoflagellate cyst taxa in surface sediments of the Northern Hemisphere in relation to environmental parameters: The new n= 1968 database. *Marine Micropaleontology*, 159, 101796. https://doi.org/10.1016/j.marmicro.2019.101796
- Divine, D. V., Korsnes, R., & Makshtas, A. P. (2004). Temporal and spatial variation of shore-fast ice in the Kara Sea. *Continental Shelf Research*, 24, 1717–1736. https://doi.org/10.1016/j.csr.2004.05.010
- Dukhovskoy, D., Johnson, M., & Proshutinsky, A. (2006). Arctic decadal variability from an idealized atmosphere-ice-ocean model: 1. Model description, calibration, and validation. *Journal of Geophysical Research*, 111, C06029. https://doi.org/10.1029/2004jc002821
- Fahl, K., & Nöthig, E.-M. (2007). Lithogenic and biogenic particle fluxes on the Lomonosov Ridge (central Arctic Ocean) and their relevance for sediment accumulation: Vertical vs. lateral transport. Deep Sea Research Part I: Oceanographic Research Papers, 54(8), 1256–1272. https:// doi.org/10.1016/j.dsr.2007.04.014
- Fahl, K., & Stein, R. (2012). Modern seasonal variability and deglacial/holocene change of central Arctic Ocean Sea-ice cover: New insights from biomarker proxy records. Earth and Planetary Science Letters, 351, 123–133. https://doi.org/10.1016/j.epsl.2012.07.009
- Fernandes, M.-B., & Sicre, M.-A. (2000). The importance of terrestrial organic carbon inputs on Kara Sea shelves as revealed by n-alkanes, OC and δ¹³C values. Organic Geochemistry, 31, 363–374. https://doi.org/10.1016/S0146-6380(00)00006-1
- Gillett, N. P., Kirchmeier-Young, M., Ribes, A., Shiogama, H., Hegerl, G. C., Knutti, R., et al. (2021). Constraining human contributions to observed warming since the pre-industrial period. *Nature Climate Change*, 11, 207–212. https://doi.org/10.1038/s41558-020-00965-9
- Gordeev, V. V., Martin, J. M., Sidorov, I. S., & Sidorova, M. V. (1996). A reassessment of the Eurasian river input of water, sediment, major
- elements, and nutrients to the Arctic Ocean. *American Journal of Science*, 296, 664–691. https://doi.org/10.2475/ajs.296.6.664
 Grebmeier, J. M., Cooper, L. W., Feder, H. M., & Sirenko, B. I. (2006). Ecosystem dynamics of the Pacific-influenced Northern bering and
- Chukchi seas in the Amerasian Arctic. *Progress in Oceanography*, 71, 331–361. https://doi.org/10.1016/j.pocean.2006.10.001
 Haine, T. W., Curry, B., Gerdes, R., Hansen, E., Karcher, M., Lee, C., et al. (2015). Arctic freshwater export: Status, mechanisms, and prospects.
- Global and Planetary Change, 125, 13–35. https://doi.org/10.1016/j.gloplacha.2014.11.013

 Hill, V., Ardyna, M., Lee, S. H., & Varela, D. E. (2018). Decadal trends in phytoplankton production in the Pacific Arctic region from 1950 to 2012. Deep Sea Research Part II: Topical Studies in Oceanography, 152, 82–94. https://doi.org/10.1016/j.dsr2.2016.12.015
- Hillaire-Marcel, C., & de Vernal, A. (2008). Stable isotope clue to episodic sea ice formation in the glacial North Atlantic. Earth and Planetary
- Science Letters, 268, 143–150. https://doi.org/10.1016/j.epsl.2008.01.012

 Holmes, R. M., McClelland, J. W., Peterson, B. J., Tank, S. E., Bulygina, E., Eglinton, T. I., et al. (2011). Seasonal and annual fluxes of nutrients and organic matter from large rivers to the Arctic Ocean and surrounding seas. Estuaries and Coasts, 35(2), 369–382, https://doi.org/10.1007/
- and organic matter from large rivers to the Arctic Ocean and surrounding seas. Estuaries and Coasts, 35(2), 369–382. https://doi.org/10.1007/s12237-011-9386-6
- Hörner, T., Stein, R., Fahl, K., & Birgel, D. (2016). Post-glacial variability of sea ice cover, river run-off and biological production in the western Laptev Sea (Arctic Ocean)—A high-resolution biomarker study. *Quaternary Science Reviews*, 143, 133–149.
- Koch, C. W., Cooper, L. W., Grebmeier, J. M., Lalande, C., Brown, T. A., & Grebmeier, J. M. (2020). Seasonal and latitudinal variations in sea ice algae deposition in the Northern Bering and Chukchi Seas determined by algal biomarkers. *PLoS One*, 15(4), e0231178. https://doi. org/10.1371/journal.pone.0231178
- Kolling, H. M., Stein, R., Fahl, K., Sadatzki, H., Vernal, A., & Xiao, X. (2020). Biomarker distributions in (Sub)-Arctic surface sediments and their potential for sea ice reconstructions. *Geochemistry, Geophysics, Geosystems*, 21(10), e2019GC008629. https://doi.org/10.1029/2019gc008629
- Köseoğlu, D., Belt, S. T., Smik, L., Yao, H., Panieri, G., & Knies, J. (2018). Complementary biomarker-based methods for characterising Arctic sea ice conditions: A case study comparison between multivariate analysis and the PIP25 index. *Geochimica et Cosmochimica Acta*, 222, 406–420. https://doi.org/10.1016/j.gca.2017.11.001
- Kraberg, A. C., Druzhkova, E., Heim, B., Loeder, M. J. G., & Wiltshire, K. H. (2013). Phytoplankton community structure in the Lena Delta (Siberia, Russia) in relation to hydrography. *Biogeosciences*, 10(11), 7263–7277. https://doi.org/10.5194/bg-10-7263-2013
- Lewis, K. M., & Arrigo, K. R. (2020). Ocean Color Algorithms for estimating chlorophyll a, CDOM absorption, and particle backscattering in the Arctic Ocean. *Journal of Geophysical Research: Oceans*, 125(6), e2019JC015706. https://doi.org/10.1029/2019JC015706

SU ET AL. 12 of 14



- Li, L., Liu, Y., Wang, X., Hu, L., Yang, G., Wang, H., et al. (2020). Early diagenesis and accumulation of redox-sensitive elements in East Siberian Arctic shelves. *Marine Geology*, 429, 106309. https://doi.org/10.1016/j.margeo.2020.106309
- Locarnini, R. A., Mishonov, A. V., Antonov, J. I., Boyer, T. P., Garcia, H. E., Baranova, O. K., et al. (2013). In S. Levitus, & A. Mishonov Technical (Eds.), World Ocean Atlas 2013, volume 1: Temperature. NOAA Atlas NESDIS (Vol. 73, p. 40).
- Massé, G., Rowland, S. J., Sicre, M.-A., Jacob, J., Jansen, E., & Belt, S. T. (2008). Abrupt climate changes for Iceland during the last millennium: Evidence from high resolution sea ice reconstructions. Earth and Planetary Science Letters, 269, 565–569. https://doi.org/10.1016/j.epsl 2008 03 017
- Moline, M. A., Karnovsky, N. J., Brown, Z., Divoky, G. J., Frazer, T. K., Jacoby, C. A., et al. (2008). High latitude changes in ice dynamics and their impact on polar marine ecosystems. Annals of the New York Academy of Sciences, 1134, 267–319. https://doi.org/10.1196/annals.1439.010
- Morison, J., Kwok, R., Peralta-Ferriz, C., Alkire, M., Rigor, I., Andersen, R., & Steele, M. (2012). Changing Arctic Ocean freshwater pathways. Nature, 481(7379), 66–70. https://doi.org/10.1038/nature10705
- Morris, K., Li, S., & Jeffries, M. (1999). Meso- and microscale Sea-ice motion in the East Siberian Sea as determined from ERS-1 SAR data. Journal of Glaciology, 45, 370–383. https://doi.org/10.3189/s0022143000001878
- Müller, J., Wagner, A., Fahl, K., Stein, R., Prange, M., & Lohmann, G. (2011). Towards quantitative sea ice reconstructions in the northern North Atlantic: A combined biomarker and numerical modelling approach. Earth and Planetary Science Letters, 306, 137–148. https://doi. org/10.1016/j.epsl.2011.04.011
- Münchow, A., Weingartner, T. J., & Cooper, L. W. (1999). The summer hydrography and surface circulation of the East Siberian Shelf Sea. *Journal of Physical Oceanography*, 29(9), 21672–22182. https://doi.org/10.1175/1520-0485(1999)029<2167:TSHASC>2.0
- Nair, A., Mohan, R., Crosta, X., Manoj, M. C., Thamban, M., & Marieu, V. (2019). Southern Ocean sea ice and frontal changes during the Late Quaternary and their linkages to Asian summer monsoon. *Quaternary Science Reviews*, 213, 93–104. https://doi.org/10.1016/j. quascirev.2019.04.007
- Nelson, D. B., & Sachs, J. P. (2014). The influence of salinity on D/H fractionation in dinosterol and brassicasterol from globally distributed saline and hypersaline lakes. Geochimica et Cosmochimica Acta, 133, 325–339. https://doi.org/10.1016/j.gca.2014.03.007
- Nöthig, E. M., Lalande, C., Fahl, K., Metfies, K., Salter, I., & Bauerfeind, E. (2020). Annual cycle of downward particle fluxes on each side of the Gakkel Ridge in the central Arctic Ocean. *Philosophical Transactions of the Royal Society A*, 378, 20190368. https://doi.org/10.1098/rsta.2019.0368
- Osadchiev, A., Silvestrova, K., & Myslenkov, S. (2020). Wind-Driven coastal upwelling near large river deltas in the Laptev and East-Siberian Seas. *Remote Sensing*, 12(5), 844. https://doi.org/10.3390/rs12050844
- Osadchiev, A. A., Pisareva, M. N., Spivak, E. A., Shchuka, S. A., & Semiletov, I. P. (2020). Freshwater transport between the Kara, Laptev, and East-Siberian seas. *Scientific Reports*, 10(1), 13041. https://doi.org/10.1038/s41598-020-70096-w
- Overland, J. E., & Wang, M. (2013). When will the summer Arctic be nearly sea ice free? Geophysical Research Letters, 40(10), 2097–2101. https://doi.org/10.1002/grl.50316
- Park, H., Watanabe, E., Kim, Y., Polyakov, I., Oshima, K., Zhang, X. D., et al. (2020). Increasing riverine heat influx triggers Arctic sea ice decline and oceanic and atmospheric warming. *Science Advances*, 6(45), eabc4699. https://doi.org/10.1126/sciadv.abc4699
- Parkinson, C. L., Cavalieri, D. J., Gloersen, P., Zwally, H. J., & Comiso, J. C. (1999). Arctic sea ice extents, areas, and trends, 1978–1996. Journal of Geophysical Research, 104(C9), 20837–20856. https://doi.org/10.1029/1999JC900082
- Petrova, V. I., Batova, G. I., Zinchenko, A. G., Kursheva, A. V., & Narkevskiy, N. V. (2004). The East Siberian Sea: Distribution, sources, and burial of organic carbon. In R. Stein, & R. W. Macdonald (Eds.), *The organic carbon cycle in the Arctic Ocean* (pp. 204–212). Springer-Verlag.
- Peulvé, S., Sicre, M.-A., De Leeuw, J. W., Baas, M., & Saliot, A. (1996). Molecular characterization of suspended and sedimentary organic matter in an Arctic delta. *Limnology & Oceanography*, 4, 488–497. https://doi.org/10.4319/lo.1996.41.3.0488
- Polyakov, I. V., Alekseev, G. V., Bekryaev, R. V., Bhatt, U. S., Colony, R., Johnson, M. A., et al. (2003). Long-term ice variability in Arctic marginal seas. *Journal of Climate*, 162(12), 2078–2085. https://doi.org/10.1175/1520-0442(2003)016<2078:liviam>2.0.co;2
- Ren, J., Chen, J., Bai, Y., Sicre, M.-A., Yao, Z., Lin, L., et al. (2020). Diatom composition and fluxes over the Northwind Ridge, western Arctic Ocean: Impacts of marine surface circulation and sea ice distribution. *Progress in Oceanography*, 186, 102377. https://doi.org/10.1016/j. pocean.2020.102377
- Rigor, I. G., & Wallace, J. M. (2004). Variations in the age of Arctic sea-ice and summer sea-ice extent. Geophysical Research Letters, 31(9), L09401. https://doi.org/10.1029/2004gl019492
- Salvadó, J. A., Tesi, T., Sundbom, M., Karlsson, E., Kruså, M., Semiletov, I. P., et al. (2016). Contrasting composition of terrigenous organic matter in the dissolved, particulate and sedimentary organic carbon pools on the outer East Siberian Arctic Shelf. *Biogeosciences*, 13, 6121–6138. https://doi.org/10.5194/bg-13-6121-2016
- Shindell, D., & Faluvegi, G. (2009). Climate response to regional radiative forcing during the twentieth century. *Nature Geoscience*, 2(4), 294–300. https://doi.org/10.1038/ngeo473
- Sicre, M.-A., Ternois, Y., Paterne, M., Martinez, P., & Bertrand, P. (2001). Climatic changes in the upwelling region off Cap Blanc, NW Africa, over the last 70 kyear: A multi-biomarker approach. Organic Geochemistry, 32(8), 981–990. https://doi.org/10.1016/S0146-6380(01)00061-4
- Smik, L., Belt, S. T., Lieser, J. L., Armand, L. K., & Leventer, A. (2016). Distributions of highly branched isoprenoid alkenes and other algal lipids in surface waters from East Antarctica: Further insights for biomarker-based paleo sea-ice reconstruction. *Organic Geochemistry*, 95, 71–80. https://doi.org/10.1016/j.orggeochem.2016.02.011
- Smik, L., Cabedo-Sanz, P., & Belt, S. T. (2016). Semi-quantitative estimates of paleo Arctic sea ice concentration based on source-specific highly branched isoprenoid alkenes: A further development of the PIP25 index. Organic Geochemistry, 92, 63–69. https://doi.org/10.1016/j. orggeochem.2015.12.007
- Sparkes, R. B., Doğrul Selver, A., Gustafsson, Ö., Semiletov, I. P., Haghipour, N., Wacker, L., et al. (2016). Macromolecular composition of terrestrial and marine organic matter in sediments across the East Siberian Arctic Shelf. *The Cryosphere*, 10(5), 2485–2500. https://doi. org/10.5194/TC-10-2485-2016
- Speer, L., Nelson, R., Casier, R., Gavrilo, M., Quillfeldt, C. v., Cleary, J., et al. (2017). Natural marine World heritage in the Arctic Ocean, report of an expert workshop and review process (p. 1–112). IUCN.
- Stein, R. (2008). Arctic Ocean sediments: Processes, proxies, and paleoenvironment. Developments in marine geology. Elsevier. 2: iii. https://doi.org/10.1016/S1572-5480(08)00014-6
- Stein, R., & Fahl, K. (2000). Holocene accumulation of organic carbon at the Laptev Sea continental margin (Arctic Ocean): Sources, pathways, and sinks. *Geo-Marine Letters*, 20, 27–36. https://doi.org/10.1007/s003670000028
- Stein, R., & Fahl, K. (2004a). The Laptev Sea: Distribution, sources, variability and burial of organic carbon. In R. Stein, & R. W. Macdonald (Eds.), *The organic carbon cycle in the Arctic Ocean* (pp. 213–237). Springer-Verlag.

SU ET AL. 13 of 14



- Stein, R., & Fahl, K. (2004b). The Kara Sea: Distribution, sources, variability and burial of organic carbon. In R. Stein, & R. W. Macdonald (Eds.), The organic carbon cycle in the Arctic Ocean (pp. 237–266). Springer-Verlag.
- Stein, R., Fahl, K., Gierz, P., Niessen, F., & Lohmann, G. (2017). Arctic Ocean sea ice cover during the penultimate glacial and the last interglacial. *Nature Communications*, 8(1), 373. https://doi.org/10.1038/s41467-017-00552-1
- Stein, R., Fahl, K., & Müller, J. (2012). Proxy reconstruction of Arctic Ocean sea ice history: From IRD to IP25, Polarforschung, 82, 37-71. https://doi.org/10.10013/epic.41492
- Stein, R., Fahl, K., Schreck, M., Knorr, G., Niessen, F., Forwick, M., et al. (2016). Evidence for ice-free summers in the late Miocene central Arctic Ocean. *Nature Communications*, 7, 11148. https://doi.org/10.1038/ncomms11148
- Stein, R., & Macdonald, R. W. (2004). The organic carbon cycle in the Arctic Ocean. Springer.
- Stocker, T. F., Qin, D., Plattner, G.-K., Tignor, M., Allen, S. K., Boschung, J., et al. (2013). Climate change 2013: The physical science basis. Contribution of working group I to the fifth assessment report of the intergovernmental panel on climate change (pp. 1–1535). Cambridge University Press.
- Stoynova, V., Shanahan, T. M., Hughen, K. A., & de Vernal, A. (2013). Insights into circum-Arctic sea ice variability from molecular geochemistry. *Quaternary Science Reviews*, 79, 63–73. https://doi.org/10.1016/j.quascirev.2012.10.006
- Tesi, T., Semiletov, I., Hugelius, G., Dudarev, O., Kuhry, P., & Gustafsson, Ö. (2014). Composition and fate of terrigenous organic matter along the Arctic land-ocean continuum in East Siberia: Insights from biomarkers and carbon isotopes. *Geochimica et Cosmochimica Acta*, 133, 235–256. https://doi.org/10.1016/j.gca.2014.02.045
- Thompson, D. W. J., & Wallace, J. M. (1998). The Arctic Oscillation signature in the wintertime geopotential height and temperature fields. Geophysical Research Letters, 25(9), 1297-1300. https://doi.org/10.1029/98g100950
- Volkman, J. K. (1986). A review of sterol markers for marine and terrigenous organic matter. Organic Geochemistry, 9(2), 83–99. https://doi.org/10.1016/0146-6380(86)90089-6
- Vonk, J. E., Sánchez-García, L., Van Dongen, B., Alling, V., Kosmach, D., Charkin, A., et al. (2012). Activation of old carbon by erosion of coastal and subsea permafrost in Arctic Siberia. Nature, 489, 137–140. https://doi.org/10.1038/nature11392
- Wang, Y., Bi, H., Huang, H., Liu, Y., Liu, Y., Liang, X., et al. (2019). Satellite-observed trends in the Arctic sea ice concentration for the period 1979–2016. *Journal of Oceanology and Limnology*, 37(1), 18–37. https://doi.org/10.1007/s00343-019-7284-0
- Weingartner, T. J., Danielson, S., Sasaki, Y., Pavlov, V. & Kulakov, M. (1999). The Siberian coastal current: A wind- and buoyancy-forced Arctic coastal current. *Journal of Geophysical Research* 104(C12), 29697-29713. https://doi.org/10.1029/1999jc900161
- Williford, K. H., Ward, P. D., Garrison, G. H., & Buick, R. (2007). An extended organic carbon-isotope record across the Triassic–Jurassic boundary in the Queen Charlotte Islands, British Columbia, Canada. *Palaeogeography, Palaeoclimatology, Palaeoecology*, 244(1–4), 290–296. https://doi.org/10.1016/j.palaeo.2006.06.032
- Woodgate, R. A., Aagaard, K., & Weingartner, T. J. (2005). Monthly temperature, salinity, and transport variability of the Bering Strait through flow. Geophysical Research Letters. 32, L04601, https://doi.org/10.1029/2004g1021880
- Wu, J., Stein, R., Fahl, K., Syring, N., Nam, S.-I., Hefter, J., et al. (2020). Deglacial to Holocene variability in surface water characteristics and major floods in the Beaufort Sea. Communications Earth and Environment, 1, 27. https://doi.org/10.1038/s43247-020-00028-z
- Xiao, X., Fahl, K., Müller, J., & Stein, R. (2015). Sea-ice distribution in the modern Arctic Ocean: Biomarker records from trans-Arctic Ocean surface sediments. Geochimica et Cosmochimica Acta, 155, 16–29. https://doi.org/10.1016/j.gca.2015.01.029
- Xiao, X., Fahl, K., & Stein, R. (2013). Biomarker distributions in surface sediments from the Kara and Laptev seas (Arctic Ocean): Indicators for organic-carbon sources and sea-ice coverage. Quaternary Science Reviews, 79, 40–52. https://doi.org/10.1016/j.quascirev.2012.11.028
- Xiao, X., Stein, R., & Fahl, K. (2015). MIS 3 to MIS 1 temporal and LGM spatial variability in Arctic Ocean sea ice cover: Reconstruction from biomarkers. *Paleoceanography*, 30(7), 969–983. https://doi.org/10.1002/2015pa002814
- Yu, Y., Stern, H., Fowler, C., Fetterer, F., & Maslanik, J. (2014). Interannual variability of Arctic landfast ice between 1976 and 2007. *Journal of Climate*, 27(1), 227–243. https://doi.org/10.1175/jcli-d-13-00178.1
- Zernova, V. V., Nöthig, E. M., & Shevchenko, V. P. (2000). Vertical microalga flux in the northern Laptev Sea (from the data collected by the yearlong sediment trap). *Oceanology*, 40(6), 801–808.
- Zhang, Y., Zhang, Y.-Y., Xu, D.-Y., Chen, C.-S., Shen, X.-Y., Hu, S., et al. (2021). Impacts of atmospheric and oceanic factors on monthly and interannual variations of polynya in the East Siberian Sea and Chukchi Sea. Advances in Climate Change Research, 12, 527–538. https://doi.org/10.1016/j.accre.2021.07.005
- Zonn, I. S., Kostianoy, A. G., & Semenov, A. V. (2016). Siberian polynya, great Siberian polynya. In *The eastern Arctic seas Encyclopedia* (pp. 307). Springer International Publishing.
- Zweng, M. M., Reagan, J. R., Antonov, J. I., Locarnini, R. A., Mishonov, A. V., Boyer, T. P., et al. (2013). In S. Levitus, A. Mishonov, & Technical (Eds.), World Ocean Atlas 2013, volume 2: Salinity (Vol. 74, p. 1–39). NOAA Atlas NESDIS.

SU ET AL. 14 of 14